CHAPTER 3

PHENOMENOLOGY OF UNDERGROUND NUCLEAR EXPLOSIONS IN ROCK SALT

YU.V. DUBASOV
RPA "V.G. Khlopin Radium Institute"
28, 2-nd Murinskii av., St-Petersburg, 194021
Russia

Abstract: Results from investigations of numerous cavities made from underground nuclear explosions conducted in rock salt in the USSR are presented. A physical-chemical model of these nuclear explosions that are based on these investigations has been developed. Problems associated with rock salt evaporation and melting, the cavity temperature regime, progress of rock salt cooling and the distribution of radionuclides in a formed cavity have been described by such model. Scientific problems arising during cavities opening and during preparations for operations have been considered. In addition, problems associated with both radionuclide migration with ground waters and contamination of radioactive products stored in the explosion cavities, are considered.

Keywords: radioactive particles, nuclear weapon tests, Semipalatinsk test site

1. Introduction

The first underground nuclear explosion (UNE) in rock salt formation was conducted in 1961 near Karlsbad, New Mexico, USA. Important program on UNE was initiated in the Soviet Union in 1966. The goal of this program was both technology elaboration to obtain transuranium and transplutonium radionuclides in weighable amounts, and the technology of creating cavities as capacities for hydrocarbon raw materials. On the whole, 40 UNEs were conducted in rock salt in the USSR. Most of explosions were conducted in vertical holes, and seven explosions were performed in cavities created by previous explosions. Thus, in the A-2 explosion cavity filled with water, six low-yield explosions were conducted with the aim to develop transplutonium elements obtaining technology. One explosion with a yield of 10 kt was conducted in the A-III explosion cavity.

The goal of this explosion was to develop a technology of multiplied explosions in one cavity, to obtain a man-made transuranium elements deposit, as well as for checking the possibility of seismic signal relaxing (decoupling) during the explosion in a

B. Salbu and L. Skipperud (eds.), *Nuclear Risk in Central Asia.*

high volume capacity. Explosions in rock salt were conducted at the sites “Galit” near the settlement Bol`shoy Azgir, at the site “Lira” (6 explosions) near Uralsk city, Republic of Kazakhstan, at the site “Vega” near the settlement “Aksaraiskay” in Astrakhan province (15 explosions), and also at the sites “Magistral” and “Sapfir” in Orenburg province (3 explosions), Russian Federation.

The earliest explosions in the USSR were conducted at the “Galit” site. These explosions were investigated most detailed. Therefore, having in mind the phenolmenology of UNE in rock salts, we were guided mostly by using the data obtained at this site, and also by some data published from the Gnome and Salmon explosions which had been conducted in USA.

2. Phases of Nuclear Explosion in Rock Salts

Long-term investigations of the central zones of underground nuclear explosions as well as calculative-theoretical investigations made it possible to create a physical-chemical model of the underground nuclear explosion. It deals with three stages of the explosion transition:

- Chemical bonds destruction and transitions of the first kind and with energy absorption
- Chemical reactions and transitions of the first kind and energy release
- Migration stage.

The first stage includes chemical decomposition of the substances, nuclear charge materials and a part of the surroundings to high-temperature (5,000–10,000 K) vapour gas mixture, and to the volume-up to practically full ionized plasma, adiabatic explosion of cavity gas, rock melting and its heating up to the temperatures, resulting in chemical changes. Thus, at this state of an explosion, significant break of chemical bonds and transfer into ion-atomic state occurs in the central plasma zone of explosion (fire ball), as well as full substance evaporation with a transfer into atomic-molecular state in the evaporation zone, melting of rock with partial decomposition, and volatile and gaseous disintegration product separation, and, finally, rock heating accompanied by crystal-hydrate destruction and volatile products giving up in the zone of thermal effect. These stages are often overlapping in space and time. The duration of the first stage of process in an ideal case is not more than some seconds.

After the descent of a special nuclear explosive device into a hole, stemming complex was mounted above this device, preventing radionuclides to escape from the hole to the day surface. During nuclear explosion huge energy emission occurs in about 0.1 μsec. The values of arising temperature and pressure could be calculated from formulae given below [1]

$$E_{tot} = E_{tot} = 3/2 \frac{6,023 \cdot 10^{23}}{M} \ldots\ kT, + 7\ 67 \cdot 10^{-15} T^{-4} = 1,25 \cdot 10^{8} \rho/\mathrm{MT} + 7,67 \cdot 10^{-15}\ \mathrm{T}^4\ \mathrm{erg/cm}^3 \quad (1)$$

where ρ = substance density, M = molecular weight of the substance, k = Boltsman constant. The total pressure of an ideal gas at high temperatures is equal to:

$$P_{tot} = 2/3\ E_{kin} + 1/3\ E_{rad} = nkT + 1/3\sigma_R T^4, \quad (2)$$

where E_{kin}= kinetic energy, E_{rad} = radiation energy, and σ_R= Stephan-Boltsman constant.

For an explosion yield of 100 kt; weight 5 t and density 2.12 g/cm^3 the temperature in the charge volume will be 1.4×10^7 K [1]. Gas pressure and radiation pressure will be 1,200 Mbar and 75 Mbar, respectively. At such high temperatures, the substance of a charge will convert into highly ionized gas, and the thermal wave will spread in the surroundings. After temperature decreases to 300,000 K, the thermal wave will transit into a powerful shocking wave, a rock salt pressure and the system is transferred into evaporated state.

The second phase includes a period and space of cooling substances in the course of adiabatic expansion, thermal- and mass-exchange when in contact with cavity walls and joints' surface. In fact, it starts in some hundreds of fractions of a second with the appearance of non-condensing gases and clusters' formation (100–200 atoms and molecules) of the most refractory elements and compounds, which is thermodynamically possible in a given mixture of elements, and is completed by gas structure stabilization and rock melt crystallization, fixing basic part of explosion radionuclides with partial restoring of the former minerals and formation of new ones. Suitable space-time stage limit is water vapours condensation that is cooling down the cavity gas and rock to 373 K.

As a cavity size increases, adiabatic expansion and cooling of ionized gas of evaporated rock take place. It results first in ions recombination; for Na and Cl atoms first the recombination into NaCl molecules and then to recombination of ionized molecules $NaCl^+$ with electrons. Recombination energy liberated here is transferred to cavity walls, that is, melted rock, which at this period still covers the walls of the cavity.

At the expense of radiance and convective heat exchange the evaporated rock temperature decreases, while this rock is still a fire ball, and NaCl condensation process begins. Latent condensation (evaporation) heat for sodium chloride is ΔH = 1 Mcal/kg (4.19 MJ/kg) and is spent on melting and heating of melted rock. With due regard to the fact that 100–110 t of rock salt are condensed, the total amount of liberated condensation heat comprises a significant part from the total explosion energy.

Under conditions of shock compression, rock salt will be evaporated, if inner energy accumulated as a result of compression, E_{evap}, is higher than 8.9 kcal/kg, and that for melting –3.4 kcal/kg [2]. These values are 2–3 times higher than under ordinary conditions (normal pressure). The shocking wave amplitude, when rock salt evaporation takes place at the front of shocking wave, is P = 0.86 Mbar (86 GPa). When the shock wave amplitude is diminished to 800 kbar pressure, the rock behind the front of shocking wave melts. When the shocking wave amplitude is diminishing to 400–500 kbar, compressed rock is crushed and heated.

Thus, in course of underground nuclear explosions, evaporation and melting of rock at the front of shocking wave take place at first, rock melts also during a relief (decompressing) of compressed rock, transforming into shock melt. Complementary melting of rock (thermally formed melt) by a previously heated shocking wave occurs at

the expense of latent heat in evaporated rock condensation, and mixture of these two melt generations results in a final radioactive melt formation.

Formation of sodium chloride vapours, main component of rock salt condensation, can take place in wide time interval. For instance, in case of water penetration from higher horizons into a cavity of small explosion (1 kt), condensation ended in 10 sec, for an explosion of 25 kt of yield condensation time was ~50 sec. In case of contained cavity rock condensation after an explosion of about 60 kt of power, rock condensation ceased in 4–6 min. These assessments were obtained by radionuclide chronometry method. The average melt temperature 100 sec after the A-I explosion was 1,800°C. In the periphery zone of the A-I explosion cavity, the temperature 10–15 sec after the explosion was 1,550–1,600°C; at the boundary of the melted rock with cavity walls the temperature reached 900–1,000°C, which resulted in additional rock melting. Melted rock in the first period after an explosion (1–2 min) contains 58% of the explosion energy that is 2.44 TJ/kt as thermal energy. Specific thermal energy in melted rock is 2.44 MJ/kg.

Solidification time (crystallization) of melts depends on many factors, in particular on water penetration into a cavity. Thus, for a series of explosions at the "Galit" site water penetration and early melt solidification in upper layers were observed for instance 10 min after the A-I explosion. Despite a high specific activity of solidified melt, it was not melted again under the influence of radiation loadings.

As a result of the powerful initial impulse received by the rock, and also of evaporated rock pressure, cavity formation and its subsequent growth takes place. Numerical calculations show that a cavity is compressed after maximum radius is achieved, and then it is expanded again, that is, up to complete stop of the cavity growth, pulsation occurs [3]. For example, the calculated cavity of "Salmon" explosion 0.1 sec after explosion had a maximum radius of 23 m, and 0.25 sec after the explosion the pulsation cavity expansion was finished, and its final radius was 22 m. Because of imperfection in the calculation technique, the theoretical radius appeared to be larger than a real one – 17.4 ± 0.6 m.

Numerical calculations of nuclear explosion cavity growth at the depth of 833 m and at a yield of 5.3 kt, that is, similar to "Salmon" explosion, were made by V.B. Adamsky and his colleagues. These calculations are presented in Fig. 1. It is seen that the cavity reaches its maximum size of 29 m, ~0,15 sec after the explosion, and then the size is reduced. Full stop of the cavity growth occurs ~0.45–0.5 sec after explosion. Compared to the estimate, the cavity radius was 19.5 m, which is 2 m larger than a real one. Estimations for the A-III and A-IV explosions with similar yields were also made. Expected cavity radius for the explosions was ~40 m, solidified melt level was located 20–25 m from the cavity centre. It is evident, that the calculated radius was in good agreement with the experimental value (38–39 m).

Final cavity radius R and volume V_{cav} can be estimated by means of equations suggested by V. Adamsky and colleagues [4]:

$$R_{м} = 14{,}5\, W_{кт}^{1/3}\,(1-\frac{H}{H_{O}})\,, \tag{3}$$

$$V_{cav} = 12800\,(1-H/2800)^{3}\cdot W,\ м^{3} \tag{4}$$

where H_o = 2,800 m; W = explosion yield, kt; H = depth of charge location.

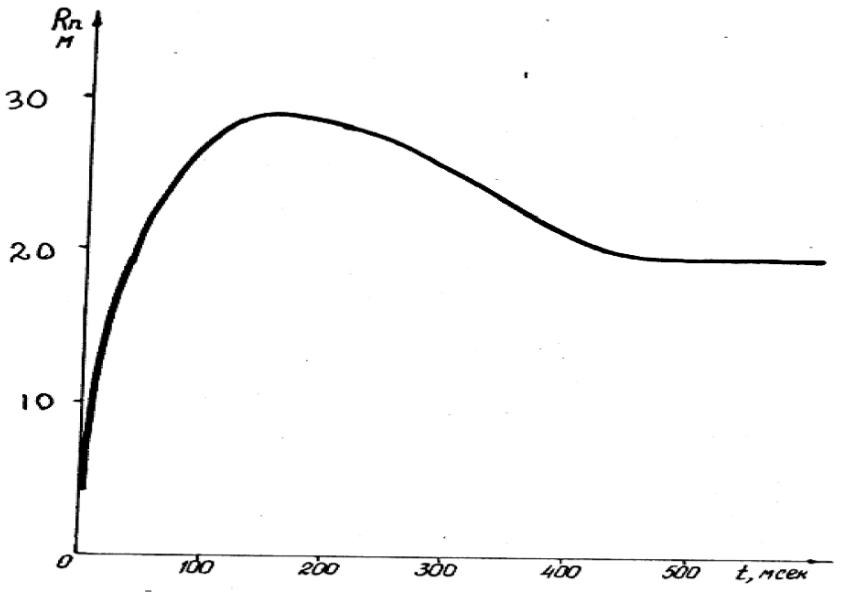

Figure 1. Numerical calculations of the nuclear explosion cavity growth at the depth of 833 m and yield of 5.3 kt

3. Mass of Evaporated and Melted Rock

Masses of evaporated and melted rock are very important characteristics of underground nuclear explosions. They were estimated by US specialists on the basis of hydrodynamic numerical calculations and by our experimental and empirical experiences. According to data from Butkovich [5], the mass of evaporated rock salt is 107 t/kt (24 t/TJ). Our estimations were based on the chemical and radiochemical structure of condensation particles, formed from chemical elements of evaporated rock and charge materials. This estimation was made from results from the investigations of A-I explosion products. According to our data, the evaporated rock mass was 108 ± 15 t/kt (26 ± 4 t/TJ), which is in good agreement with calculated values published earlier [5].

In course of the investigation of the "Gnom" and "Salmon" explosions in USA, experimental data on melted rock mass were obtained. In the "Gnom" explosion, because of a large roof caving, the melt was significantly diluted with crushed rock and completely overlapped with it. Core material obtained as a result of drilling was a mixture of dead rock and radioactive melt with different concentrations. Treatment of obtained materials made it possible for the US investigators to draw a conclusion, that during the explosion ~3,500 t of rock salt were melted, and the specific melt yield for energy liberation unit (kt) was 1,000 t/kt (240 t/TJ) [6]. In a television survey of the "Salmon" explosion, the cavity was geometrically determined from the volume of melt, which allowed the estimation of melted rock mass – 5,000 t. Specific melt mass for this

explosion was also 1,000 t/kt (240 t/TJ) [3]. Thus, it was estimated, that as a result of an underground nuclear explosion in rock salt with a nuclear explosion device located in a hole or within a small volume, rock salt melt is formed having specific mass of 1,000 t/kt (240 t/TJ).

4. Temperature in Rock Salt Melt

Experiments of Cormer and co-workers on rock salt shock compression [7] showed that the NaCl crystal melting behind the shocking wave front begins at 54 GPa, and the complete transfer into liquid state is finished at 70 GPa and temperature of 3,700 K. In the pressures interval 54–70 GPa, the temperature of the salt is practically constant because of continuing melting. According to our calculation data, during a nuclear explosion in rock salt, the peak rock temperature at the border of an evaporation zone and melting (R = 2.35 m) is ~6,000 K. In the range of temperatures below 3,200 K, the temperature drop, depending on the distance, can be presented by an analytical equation

$$T(R) = 8{,}2 \cdot 10^4 \cdot R^{-3{,}0} \tag{5}$$

From this, it can be estimated, that rock temperature at the border of zone with the mass of 1,000 t (R = 4.76 m) is 800 K. However, in the process of cavity formation and because melted rock is flowing onto the cavity bottom, heated and melted rock is intensively mixed, and temperature smoothing occurs. We managed to determine this experimentally, when investigating the rock extracted from the A-I explosion cavity. Investigation of core material from radioactive rock in the A-I explosion cavity showed that there were small spherical particles with the size of 0.05–5 mm. They had high specific activity from refractory radionuclides ^{91}Y, $^{95}Zr + {}^{95}Nb$, $^{141,144}Ce$ in the order of magnitude of $3 \cdot 10^{12}$ Bq/kg (80 Ci/kg). Spherical form of olivine slag granules formed in the rock salt melt, supported the facts, that these particles initially had a form of silicate melt drops, not mixed with the NaCl melt. Similar granules were found earlier as products from the "Gnom" explosion [8]. According to X-ray-phased and petrographic-mineralogical analysis data, the granules contained structure compounds of olivine type with different ratios of the last compounds of the series: forsterite Mg_2SiO_4-fayalite Fe_2SiO_4, montichellite $CaMgSiO_4$, periclase MgO etc. Their colour changed from white to black depending on their composition. Thus, there were forsterite, montichellite, periclase in white granules, and almost no ferric compounds.

Granules melting temperature was also measured. Depending on the composition, temperature varied in the integral from 1,800°C to 1,560°C. So, white granules with chemical composition similar to rock salt impurity composition were melting at 1,730–1,790°C. Melting temperature of MgO (20%) and forsterite Mg_2SiO_4 (80%) mixture was ~1,800°C [9], melting temperature of montichellite was 1,500°C [10]. Thus, it can be considered that the rock salt melt in the A-I nuclear explosion had a peak temperature not lower than 1,800°C. White granules with the highest melting temperature were found in salt samples from periphery zones and were in a melting state for 1–2 sec, as we determined by using radionuclide chronometry method. Basing on this fact, we came to the conclusion, that in a periphery zone the temperature was lower than

1,800°C, and in this zone the granules solidified quickly. Black granules found in the same zone, had melting (crystallization) temperature of 1,550–1,620°C and were solidified 10–15 sec after the explosion. In the central zone of the melt segment, where granules of interfered composition were found, a temperature between 1,620–1,740°C was kept for about 100 sec after explosion. Other salt impurities could also verify the temperature in peripheral zone.

Thus, in core material samples extracted from the margin zone of the lower cavity, half-spherical pieces of steel with melted edges were present, that is, it was momentary heated up to a temperature about 1,500°C. In the same zone, the compound $MgFe_2O_4$ – magnesioferrite was presented, formed as a result of explosion, while not existing at temperatures higher than 1,500°C. In a zone of melted rock in contact with cavity walls, compounds such as $CaCO_3$, MgO and γ-Ca_2SiO_4, were formed during the explosion, while their existence demonstrates that the temperature was not exceeding 900–1,000°C. Under melted rock there is a layer of recrystallized salt, that is, the salt had been heated to ~800°C. This layer is about 10 cm thick. This layer is assumed to be an initial cavity wall, melted under the influence of the heat emitted by the melt at the bottom of the cavity. Temperature distribution in melted rock segment from the A-I explosion is shown in Fig. 2.

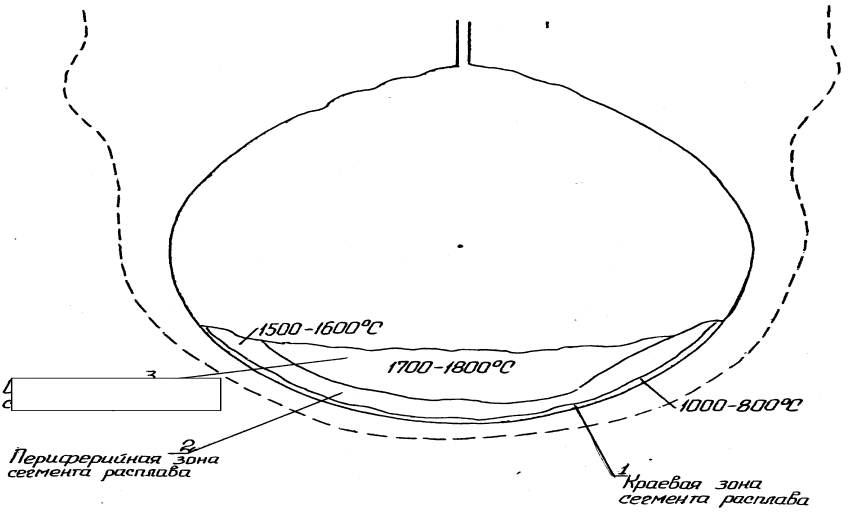

Figure 2. Temperature distribution in a melted rock segment from the A-I explosion

According to Edwards and Holzman [11], the temperature of a melt flowing down to the bottom of "Salmon" explosion crater was in the range from 2,500°C to 800°C, the average temperature of melt collected at the cavity bottom is estimated to 1,400°C [11]. Rawson and co-workers [12], assuming that the formation of compounds such as CaO and Na_2SO_4 during the "Salmon" explosion was a result of the anhydrite $CaSO_4$ reaction with NaCl

$$CaSO_4 + 2NaCl + H_2O = CaO + Na_2SO_4 + 2HCl \quad (6)$$

supported the fact, that the melt temperature during the first minutes after explosion was about 1,800°C. The rock salt melt temperature in the "Gnom" explosion was also estimated to ~1,800°C [6].

The presence of thenardite Na_2SO_4, found among the A-III-1 explosion products, demonstrates also to a reaction temperature ~1,800°C [6]. Small "balls" of melted iron were also found, as well as larger melted ferric pieces, covered by thick layer of recrystallized rock salt (black colour), under which only ferrous oxide, FeO, was found. Here, we can also speak about a peak temperature not lower than 1,800–1,500°C.

In the A-IV explosion products investigation it was stated, that in melted salt samples of dark colour Na_2SO_4 could be found. This compound did not existing before the explosion. Particles in the form of cubic well-cut crystals of magnetite Fe_3O_4, crystallized, evidently, from Fe_3O_4 melt were also found. Existence of Na_2SO_4 supports that a possible melt heating up to peak temperature was not lower than 1,800°C, and as a fact of magnetite melting – to peak temperature not lower than 1,530°C. Among the explosion products, particles of ferrosilicate slime with melting temperature of 1,220 ± 50°C were present. Particles of this compound were present in a melted state and were transported in a melt influenced by convective currents and turbulence 10–15 min after the explosion.

Thus, experimental data from five explosions, having different yields (from 1 to 60 kt), in rock salt support the facts, that rock salt melts formed during the explosions initially had an average peak temperature not lower than ~1,800°C. In the periphery melt segment zone a temperature of ~900–1,000°C was about constant.

5. Cooling Down of the Cavity

The cavity cooling regime was estimated by numerical methods for explosions, similar to the A-III and A-VI explosions 60 kt yield. Total melt volume was 27,000 m^3, and the density 1.9 g/cm^3. Temperature at the initial time moment t = 0 was estimated to 811°C, not as absolute explosion time, but time of counting "the beginning". According to our data, the melt in the A-I explosion cavity solidified 8–10 min after explosion. It occurred because of fast penetration of water into the cavity. The melt in the Salmon explosion cavity was liquid in its central part for 80–120 days.

Lens (segment) solidification begins from the surface, spreading in increasing the area. The central part of melt segment is solidified latest. The calculations were made with due regard to convection and without convection (the cooling process is slower). In the present paper, convection has been taken into consideration. Total melt crystallization in the lower part of the cavity was completed about 125 days after explosion. Cooling of the central part of melt segment started practically immediately after all melt was present in the bottom cavity. In the course of melt cooling (solidification) the massif is heated to a radius not exceeding 85 m from cavity centre (Fig. 3). Rise of the massif 's temperature to more than 100°C is observed at a distance of not more than 20 m from cavity walls. Gas void inside the explosion cavity is supposed to be isothermic, therefore a change of temperature inside the cavity is characterized by temperature dependence at melt surface over time. A cavity cooling process following a lower yield

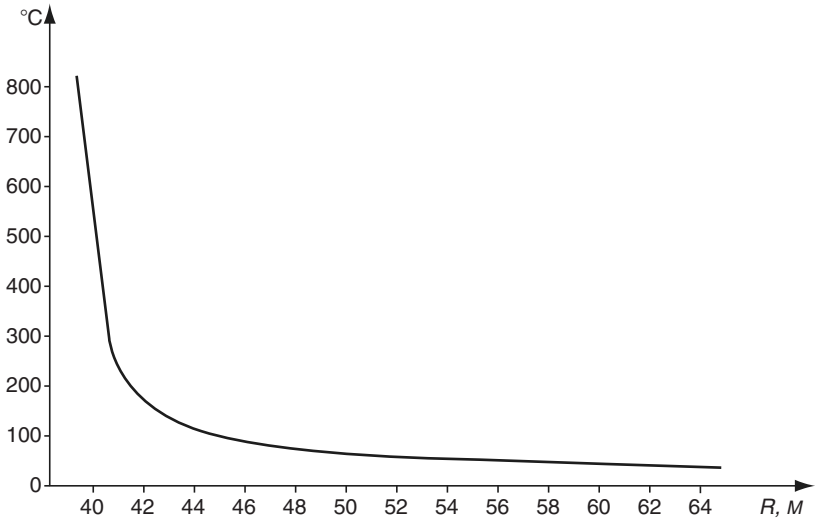

Figure 3. Rock salt temperature outside cavity of A-III-1 explosion (calculation)

explosion occurs faster. Initial moment of cavity cooling would be similar to one considered above, but with sharper temperature drops in the cavity.

Cavity cooling has also been considered following the "Salmon" explosion [12]. The initial energy distribution was as follows: 50% in the explosion cavity, more exactly, in melted salt with a temperature of 1,300°C, the remaining is beyond the limits of the cavity. Salt was kept liquid for at least 1 month; it was ascertained by the radionuclide chronometry method and data on ^{131}I and its daughter radionuclide ^{131m}Xe. In accordance with calculations [12], the final salt crystallization was completed 80-120 days after explosion in a point at a mark 3.9 ± 0.2 m below the upper melting border. About 32 months after the explosion, the "Salmon" explosion cavity temperature was 20°C higher than the natural massif temperature. Four years after the A-III and A-IV cavities opening, the temperature in the cavity was 90–95°C. Calculation of the A-III explosion cavity walls cooling is presented in Fig. 4.

The nuclear explosion energy distribution in thermal E_T and kinetic E_K in a surrounding massif can be expressed by the equation:

$$E_к = E_m - E_т = E_o - E_o(V_o/ V_1)^{\gamma-1} - E_т \quad (7)$$

where E_m is the energy transmitted to the massif, that is, initial explosion energy E_o minus the energy left in the cavity after adiabatic expansion, V_o = initial volume, V_1 = cavity volume, γ = adiabata exponent. Calculations show that thermal energy is [13]:

$$E_т = 0{,}75E_o[1 - (P_1/ P_o)^{\gamma-1}], \quad (8)$$

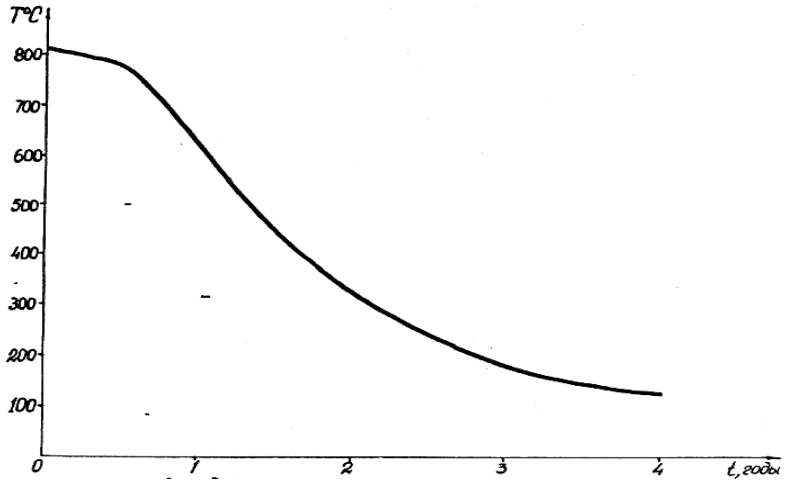

Figure 4. Calculation of A-III explosion cavity walls cooling

where P_o = initial pressure in a cavity, P_1 = threshold pressure at the shocking wave front, whose energy transmitted to the massive is discharged for phase transitions (evaporation, melting) and heating, γ = adiabata exponent. Let us consider which part of the energy is accumulated by melted rock in the initial time moment. Rock salt (NaCl) melting heat is 486 kJ/kg, and the heat capacity at 800°C is 1.09 kJ/kg and increasing with temperature growth. To simplify the calculations it was regarded that average temperature of the rock melt, when it flows down into lower half-sphere of the cavity, is 1,800°C. Multiplying the values obtained for melt masses from 1,000 t/kt, it was obtained that initially the thermal energy in the melt was 2.44 TJ ($2.44 \cdot 10^{12}$ J), that is 58% of energy for an explosion yield of 1 kt (energy liberation –4.19 TJ). Besides, thermal energy is contained in an isothermal gas and, of course, in cavity walls.

According to the calculations for the "Salmon" explosion [12], the melt having a temperature 1,300°C contained ~50% of explosion energy, the remaining 50% were exponentially distributed beyond the cavity limits with a radius of 17.4 m; ~25% were contained in the first spherical formed layer with thickness of 0.8 m, ~12.5% in the next layer of the same thickness, etc. Four months after explosion, the thermal energy distribution was: 40% above the horizontal plane crossing the cavity centre, 10% in the solidified melt zone and 50% in the lower half-sphere with a radius of ~38 m. After 32 months, the heat was diffused at the distance of nearly 60 m.

At the distance of 70 m from the explosion point, a significant rise in temperature cannot be observed. So, almost 90% of "Salmon" explosion energy was finally transferred into thermal energy and distributed in the cavity and in its vicinity having a radius about 60 m [12]. Besides, about 2% of the energy is expended for seismic wave and activities associated with the cavity expansion.

6. Radiation Effects in Rock Salt

Based on investigation of core materials collected about 0.5 month after the A-I explosion by means of a slope-horizontal hole, dense yellow-orange colour of radioactive rock salt was observed. Later, when core material from the massif located above an explosion cavity was inspected, radioactive salt was found having blue and dark-violet colour. Spectrophotometric investigations of monocrystal plates from the core materials showed yellow salt monocrystals with absorption band with wave length of $\lambda = 476$ mμ and conditioned by F-centres existence. The absorption spectrum of blue and dark-violet salt had weakly shown wide band with a maximum in an area with $\lambda = 600$ mμ (6,000 Å), conditioned by R_2-centres existence with the absorption maximum 5,960 Å and R-centres with an absorption band at 6,100 Å [14]. It is known, that F-centres are formed during rock salt crystals irradiated by X–rays or other ionizing radiation [15]. Existence time for F-centres is about 10^7 sec (3 months). The salt colour is changed to black, that is, F-centres transform into M-centres. R-centres are formed in salt irradiated at temperatures between 150–220°C or in yellow salt crystals heated up to 200°C, what was also observed under laboratory conditions.

A change in colour into dark-blue of the salt located in the massif above the explosion cavity, supports the facts that irradiation occurred at up-raised temperature. Radionuclide composition of the rock salt samples with dark-blue colour indicated the formation of joints in the rock salt massif after explosion. Along these joints radioactive noble gases, e.g., ^{89,90,91}Kr and ^{131,133,135,137}Xe were moving. As the salt in this area was irradiated at temperatures up to about 150°C, the conclusion was drawn that hot gases were moving along the joints, and also that hot water vapours formed after the first water penetrated into the A-I explosion cavity. Later coloured salt crystals were found among the radioactive salt samples withdrawn to the surface from the A-IV explosion cavity.

7. Migration Phase

The migration phase starts from the moment of cavity opening (unhermetically); it can be overlapped by the second phase and can exist, for the whole period of an explosion zone existence, as an artificial geological body and is characterized by substance recrystallization with a temperature close to geothermal ones.

Nuclear explosion with a yield of 1 kt i.e. is a consequence of instant nuclear fissions of $1.45 \cdot 10^{23}$ nuclei from ^{235}U or ^{239}Pu. In one nucleus decay, two fission fragments are formed, that is, radionuclides with different properties, mass and half-life. The spectrum of fission fragment elements is very wide: from ^{72}Zn to gadolinium ^{159}Gd. In the first minute after fission (explosion) the fission product activity is 20 GCi/kt ($8 \cdot 10^{20}$ Bq/kt). More than 90% of the activity comprises of short-lived radionuclides; radioactive noble gases (RNG) comprise 15%, and together with brome and iodine isotopes they comprise 22%. Initially all radionuclides formed in nuclear fission (fission fragments), residual nuclear fuel, induced radionuclides are together with evaporated rock in gaseous state. Pressure in an explosion cavity for the moment of cavity growth stop can be equal to litostatic pressure of overlying rocks. After the condensation of the

great bulk of rock masses, radioactive isotopes of noble gases – krypton and xenon isotopes – are contained in a gaseous phase in the cavity, together with radionuclides of highly volatile compounds, for which condensation occurs at a lower temperature (bromine, iodine, selenium, tellurium, rubidium, antimony, et al.). Radionuclides of noble gases are in principal migrating radionuclides. They can migrate along fractures in rock massif and stemming complex. Process of RNG effluent from central zones can be continued for a long time. The release of RNG depends on both stemming complex reliability and rock salt structures. However, release of gases can be a consequence of a planned technological opening of a cavity through special holes.

Releases from cavities (effluent) into the atmosphere often have two stages. Dry "cold" gas with moisture concentration of 10–20 mg/l and temperature about 20° will leave the cavity first (Table I). Then, after heating of the hole walls by vapour-gaseous mixture, the release of vapour effluent from the cavity was initiated. The most intensive vapour effluent was observed in the E-1, E-3, 2T, 3Tk, 4Tk cavities. In other cases it was mostly less intensive or insignificant. There were no vapour effluents at all from 3T, 8T, 2Tk and 6Tk cavities; and these results indicated that the outlet gases process from cavities was a one-stage process. For technological opening of cavities, pressurized water and gases were expected to be present. But in some cases, excess pressure was not observed; for instance, no excess pressure was observed during drilling of the explosion cavities in 4T, 5T, 7T, 11T (site "Vega") and 2Tk and 5Tk (site "Lira") holes. Values for initial excess pressure observed at opening of many other cavities varied between 0.02 MPa (0.2 atm) to 0.48 MPa (4.9 atm). Information on temperatures in cavities at the time of the opening was obtained by direct temperature measurement in cavities. At least in nine cavities the temperature exceeded 100°C.

TABLE I. Composition of gas effluents from cavities at "Lira" site

	Gases composition (%) (volumetric)						
Cavity	CO_2	CO	CH_4	O_2	N_2	H_2	Heavy hydro-carbons
1-TK	91	≤0.05	2.34	≤0.025	5.6	0.048	
2-TK	8.0	≤0.1	21.3	3.8	27 ÷ 73	0.5 ÷ 3.6	
3-TK	32.4	≤0.05	1.8	≤0.01	51.5	0.19	0.4
4-TK	15.7	≤0.05	3.8	≤0.01	75.7	0.12	1.0
6-TK	17.5	≤0.05	8.0	≤0.01	66.6	2.78	2.1

Scientists from V.G. Khlopin Radium Institute showed that there were at least three different types of gaseous atmosphere in the underground cavities of "Lira" site: (1) CO_2 (1-TK); (2) CO_2-N_2 with methane CH_4 impurity (3-TK, 4-TK, 6-TK; about the same gas composition from T-14 cavity of the "Vega" site); and (3) methanonitric with hydrocarbon dioxide impurities (2-TK and T-15 cavity of the "Vega" site).

Gaseous-liquid inclusions and lenses in a zone of opened fractures could also be the sources of nitrogen and methane. The major part of methane could be formed in

decomposition process of organic substances containing rock salt anhydrates layers. The chemical composition of organic compounds in vapour-gaseous mixture of "Lira" site cavities is shown in Tables II and III.

TABLE II. Composition of hydrocarbon gases from some cavities at the "Lira" site (%) (vol)

Gas	Cavities		
	3-TK	4-TK	6-TK
CH_4	1.1 ÷ 2.51	3.5 ÷ 4.2	8.1
C_2H_6	0.23 ÷ 0.37	0.63 ÷ 0.78	1.6 ÷ 1.7
C_3H_8	0.03 ÷ 0.04	0.13 ÷ 0.18	0.21 ÷ 0.27

TABLE III. Activity concentration of Krypton-85 at the "Lira" site

Explosion	^{85}Kr volumetric activity in sample ($Bq/m^3 \cdot 10^5$)
1-TK	5.7 ± 0.2
2-TK	5.4 ± 0.1
3-TK	4.0 ± 0.2
4-TK	5.8 ± 0.2

It can be seen that the major hydrocarbon components in these three cavities were: methane –1.1–8.1%, ethane –0.23–1.7%, propane –0.03–0.27%. Beside these compounds, C_3H_6, iC_4H_{10}, nC_4H_{10}, iC_5H_{12}, iC_6H_{14}, nC_6H_{14} were also present. In cavities ready for exploitation ^{85}Kr was practically not present, as it had escaped to atmosphere during the first effluent release.

Tritium, despite multiple gas exchange in the cavity, escaped into the air during repeated effluent treatments (mainly in light-volatile forms of molecular hydrogen and hydrocarbons), but not more than 10% of its total concentration in the cavity. Tritium was mainly left in the cavity and in the fissured zones in the form of HTO oxide. During rapid gas release, when the technological hole has not yet been heated sufficiently, escaped gas does not contain moisture, and tritium is in the gaseous form as HT, HTS and CH_3T. With long-time gas streaming increasing the heat, vapor appeared in the gas, and tritium was predominantly in oxidized form. Tritium was present in different forms; the distribution observed in vapor-gaseous mixture flowing from the E-3 cavity ("Magistral" site) was: HTO-90%, HT-8%, CH_3T-2%. The results of the investigation of the distribution of tritium chemical forms in vapour-gaseous mixture flowed at "Vega" site are given in Table IV.

Based on results from the investigation on the tritium concentrations and forms in vapour-gaseous mixtures in nuclear explosion cavities in salt rocks, conclusions can be drawn about tritium distribution regularities:

TABLE IV. Tritium distribution in vapour-gaseous mixture (VGM) at opening of the cavities at the "Vega" site

Explosion	Tritium volumetric activity in VGM components, Bq/l					
	HTO	HT	HTS	CH_3T	T-hydrocarbons	ΣT*
T-3	$7.4 \cdot 10^3 \div 1.8 \cdot 10^6$	$1.1 \cdot 10^5$	$7.4 \cdot 10^4$	$1.1 \cdot 10^6$	$1.5 \cdot 10^5$	$1.5 \cdot 10^6 \div 3.3 \cdot 10^6$
T-6	$7.4 \cdot 10^4 \div 3.3 \cdot 10^7$	$1.5 \cdot 10^5 \div 1.8 \cdot 10^6$	–	$7.4 \cdot 10^5 \div 3 \cdot 10^6$	–	$1.1 \cdot 10^6 \div 3.7 \cdot 10^7$
T-8	$2 \cdot 10^3$	–	$2.5 \cdot 10^4$	–	–	$2.2 \cdot 10^5$
T-14	$2.2 \cdot 10^3$	$1.85 \cdot 10^6$	$3.7 \cdot 10^4$	$2.2 \cdot 10^7$		$2.6 \cdot 10^7$

* Changes in the VGM moisture in release processes resulted in a decrease in the tritium activity concentrations. Upper and lower limits are given.

The original bulk of tritium in flowing VGM is present in a hydrocarbon form, followed by hydrogen, hydrogen sulphide and water in accordance with order of magnitude; Later, increase in the tritium concentration in VGM is observed during flowing process, basically at the expense of moisture increase in VGM, thus increasing the fraction of oxidized tritium form in the total tritium activity concentration in VGM;

The fraction of tritium in oxidized form does not significantly appear at the cavity surface and this fraction is left in the nuclear explosion cavity. This is supported by the fact, that in the VGM release process, the cavity hole plays the part of a "reversed cooler" (it does not manage to heat), and the water vapours condense and flow downwards in the cavity.

Up to now a lot of experimental data are accumulated resulting in information on production contamination stored in nuclear explosions cavities. On the basis of investigations on radionuclides distribution in systems such as salt-gaseous condensate, brine-gaseous condensate, water – methanolic brine – gaseous condensate, possible radionuclides concentrations in gaseous condensate of Orenburg gas-condensate deposit have been estimated. After more than 15 years, which had passed from the time when the first reservoir was created by exploitation, stored gaseous condensate samples have been analyzed with respect to the radionuclides concentrations.

It is evident that long-term storage of gaseous-condensates in reservoirs in contact with rock and brine containing radionuclides does not result in contamination higher than the permissible levels. However, in case of petroleum filling in underground reservoir situation becomes significantly different. Investigation on the radionuclides distribution in systems such as brine-methanol gaseous condensate – petroleum (under different conditions and phase ratios), the radionuclides concentration in organic phase can exceed the permissible levels.

As a summary, the outflow into the atmosphere of ^{85}Kr and tritium from experimental and pilot nuclear explosions with total yield 0.6 Mt, in the period after opening were: $2 \cdot 10^4$ Bq ($5 \cdot 10^3$Ci of ^{85}Kr) and ~$1.3 \cdot 10^{15}$ Bq ($3.5 \cdot 10^4$ Ci of T). The most critical factor influencing the consequences of underground nuclear explosion is the migration of radionuclides into rock massif, and, more exactly into groundwaters (Table V).

TABLE V. Expected and actual contamination levels of gaseous condensate containing radionuclides

		Volumetric activity (Ci/l) Tritium					
		Light fraction	Hard fraction	^{137}Cs	^{125}Sb	^{106}Ru	^{90}Sr
1	Forecast	$n \cdot 10^{-6}$		$N \cdot 10^{-10}$	$n \cdot 10^{-9}$	$n \cdot 10^{-9}$	$n \cdot 10^{-10}$
2	E–1÷E–3	$(1–3)\ 10^{-6}$		$<1 \cdot 10^{-10}$	$(1–10) \cdot 10^{-9}$	$(1–10) \cdot 10^{-9}$	$<1 \cdot 10^{-12}$
3	1TK	$8 \cdot 10^{-8}$	$2.2 \cdot 10^{-7}$	$1 \cdot 10^{-10}$	$<1 \cdot 10^{-8}$	$1 \cdot 10^{-8}$	$<1 \cdot 10^{-11}$
4	2TK	$5.4 \cdot 10^{-7}$		$2 \cdot 10^{-10}$	– " –	– " –	– " –
5	3TK	$5.4 \cdot 10^{-8}$	$5.4 \cdot 10^{-7}$	$1 \cdot 10^{-10}$	– " –	– " –	– " –
6	4TK	$\sim 10^{-6}$		$1 \cdot 10^{-6}$ *	$6 \cdot 10^{-8}$	–	–
	ПДК	$5.4 \cdot 10^{-4}$		$8.1 \cdot 10^{-6}$	$8.1 \cdot 10^{-5}$	$1.1 \cdot 10^{-5}$	$1.5 \cdot 10^{-7}$

*Water was present in sample as emulsion

Observations of radionuclides in groundwater at the "Galit" site for some years have shown that the level at the A-III explosion site was practically not changed (or the change was insignificant). This may indicate that radionuclides coming into groundwaters at the "Galit site", the area of technological sites except for the technological site A-I, occurred as a result of the gaseous precursors to cesium-137 (^{137}Xe) and strontium-90 (^{90}Kr) diffusion at the explosion site, indicating isolation of this water- bearing structure and slow movement rate of groundwaters. In groundwaters at the A-V sites, significant ^{131}Cs concentration was found in the groundwater sampled from the observation hole A-V-2, situated at the distance of 100 m from the main technological hole. Specific activity of ^{137}Cs in 1990 was $4.8 \cdot 10^{-10}$ Ci/l, that is, 30 times lower than PC_B. The ^{90}Sr concentration in this water reached values up to $1 \cdot 10^{-10}$ Ci/l, that is, only four times lower than PC_B for water. The tritium activity as HTO in all investigated samples from groundwater at the "Galit" sites was lower than $1 \cdot 10^4$ Bq/l, which was ten times lower then PC_B for drinking water.

Thus, on the basis of the investigations of the groundwaters activity at the "Galit" site in can be seen that ^{137}Cs and ^{90}Sr activity concentrations in observation holes around the cavities of A-II, A-III, A-IV, A-V explosions were lower than PC_B for drinking water, but somewhat higher than the contamination level of surface waters by global fallouts from atmospheric nuclear weapons tests. The exception is the cavity from the A-I explosion. Small oreols of radionuclides in groundwaters, 10 years after the explosion, demonstrate that the migration of radionuclides is still limited.

References

1. Teller E. et al. The constructive uses of nuclear explosives. McGraw-Hill, 1968.
2. Holzer F. Calculation of seismic source mechanisms. Proc. Roy. Soc., 1966, v. 290, N. 1422, pp. 408–429
3. Rawson D., Randolph P. et al. Postexplosion environment resulting from the Salmon event. J. Geoph. Res., 1966, v. 71, N. 14, pp. 3507–3521.

4. Adamsky V.B., Adymov Z.I., Akhmetov E.Z. et al. Peaceful Nuclear Explosions at Bol`shoy Azgir salt dome deposit. Annual Report of the Institute of Nuclear Physics National Nuclear Centre of Kazakhstan Republic, VNIPIPromtechnology, Almaty, 1998 (in Russian).
5. Butkovich T.R. The gas equation of state for natural materials. Lawrence Radiation Laboratory, University of California, Livermore, CA, UCRL-14729, 1967.
6. Rawson D., Boardman C., Jaffe-Chazan N. The environment created by a nuclear explosion in salt. Project Gnome, report PNE-107F, Livermore, CA, 1964.
7. Kormer S.B., Sinitsyn M.B., Kirillov G.A., Urlin V.D. Experimental determination the temperatures of shock compressed NaCl and KCl, and their curves melting up tp 700 kbar. Journal of Experimental and Theoretical Physics Letters (JETP Letters), 1965 (in Russian).
8. Kahn J.S., Smith D.K. Mineralogical investigations in the debris of the Gnome event near Carlsbad, New Mexico. Amer. Mineral., 1966, v. 51, pp. 1192–1199.
9. Griffiths P.R., Brown C.W., Lippincott E.R., Dayhoff, M.O. Termodynamic models in cosmochemical systems. Geochim. Cosmochim. Acta, 1972, v. 36, N. 2, pp. 109–129.
10. Yang J. Decomposition of solid substances kinetics, Moscow, Mir, 1969 (in Russian).
11. Edwards A.L., Holzman R.A. Thermal effects of nuclear explosion in salt. The Salmon experiment. Naturwissen, 1968, Bd. 55, N. 1, s. 18–22.
12. Rawson D.E., Taylor R.W., Springer D.L. Review of the Salmon experiment a nuclear explosion in salt. Nuturwissen, 1967, Bd. 54, N. 20, s. 525.
13. Adamsky V.B. Growth cavity by explosion and accompanying seismic effect. Issues of Atomic science and technic. Theor. Appl. Phys., issue 4, pp. 8–17, TsNIIAtomInform, M., 1991
14. Geck F.W. Zs. Naturforsch, 1957, Bd. 12a, s. 562.
15. Mott G., Gerni R. Electronic process in ionic crystals, M., 1950 (in Russian).